Dual-Wideband Filtering Power Divider With Good Isolation and High Selectivity

Citation for published version:
Wang, X, Wang, J, Zhang, G, Hong, J-S & Wu, W 2017, 'Dual-Wideband Filtering Power Divider With Good Isolation and High Selectivity', *IEEE Microwave and Wireless Components Letters*, pp. 1-3. https://doi.org/10.1109/LMWC.2017.2758318

Digital Object Identifier (DOI):
10.1109/LMWC.2017.2758318

Link:
Link to publication record in Heriot-Watt Research Portal

Document Version:
Peer reviewed version

Published In:
IEEE Microwave and Wireless Components Letters

Dual-Wideband Filtering Power Divider With Good Isolation and High Selectivity

Hong, Jia-Sheng

Published in:
IEEE Microwave and Wireless Components Letters

Publication date:
2017

Document Version
Peer reviewed version

Citation for published version (APA):
Hong, J-S. (2017). Dual-Wideband Filtering Power Divider With Good Isolation and High Selectivity. IEEE Microwave and Wireless Components Letters.

Dual-Wideband Filtering Power Divider with Good Isolation and High Selectivity

Xuedao Wang, Jianpeng Wang, Gang Zhang, Jia-Sheng Hong, *Fellow, IEEE*,
and Wen Wu, *Senior Member, IEEE*

***Abstract*—A new microstrip dual-wideband filtering power divider (FPD) is presented in this letter. The proposed device is mainly composed of a resonator loaded quarter-wavelength (λ/4) three-line coupled structure and a modified isolation network. To illustrate the design principle of the proposed FPD, equivalent circuits of the structure under the even-/odd-mode excitations are provided with the derived design equations. For demonstration, a prototype dual-band FPD operating at 2.3 GHz and 3.64 GHz with 3-dB fractional bandwidths of 36.5% and 22.3% is designed, fabricated and tested. Results indicate that the new FPD exhibits both good isolation and high frequency selectivity within the whole operation band.**

***Index Terms*—Filtering power divider, dual-wideband, high selectivity**

I. Introduction

In recent years, designing highly integrated multi-function microwave circuits has become an effective approach to meet the demands for compact and low-cost radio frequency (RF) devices. Among them, the filtering power divider (FPD) characterized with both the functions of power division/ combination and frequency selectivity has been attracting more and more attention.

Till now, many efforts have been made on exploring high performance FPDs. For instance, by replacing the quarter-wavelength transformers in conventional Wilkinson PD with the filtering sections, narrow single-band and dual-band FPDs with sharp selectivity were presented in [1]-[3]. Alternatively, study on wideband FPD with one stub-loaded ring resonator has been reported in detail [4]. On the other side, to realize single-band power dividers with various functions such as the equal, unequal, and tunable power splitting ratio, the conventional three-line coupled structure has been widely utilized in [5]-[7]. However, these works are featured without the bandpass filtering response and the port-to-port isolations need to be improved. Thus, to obtain good filtering properties, a dual-mode dual-band FPD was investigated in [8] with four stub-loaded resonators symmetrically placed at both sides of the central line. Nevertheless, large circuit area is occupied due to the adopted four dual-mode resonators. Moreover, most of the reported dual-band FPDs are focused on the narrow band operation and few of the investigations on the dual-wideband FPD have been effectively carried out.

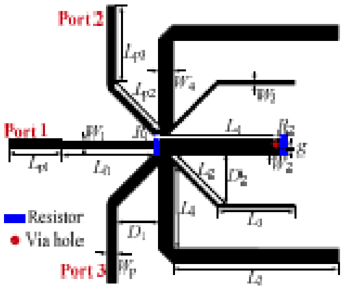

Fig. 1 Layout of the proposed dual-wideband filtering power divider (FPD).

The main motivation of this letter is to present a novel dual-wideband FPD with high frequency selectivity and good port-to-port isolation. For this purpose, a new coupling topology constructed with two open stub resonators loaded on both side lines of a three-line coupled structure is proposed. By applying specific boundary conditions caused by the resonance of the loaded stubs on the terminal of three-line coupled structure, good filtering responses have been readily obtained from the new coupling topology. Furthermore, high isolation level is successfully achieved by a modified isolation network including two isolation resistors implemented on the both two terminals of the sidelines. For demonstration, a prototype FPD centered at 2.3/3.64 GHz is designed, fabricated, and tested.

II. Design Theory of the Proposed FPD

Fig. 1 depicts the layout of the proposed FPD, which consists of a λ/4 three-line coupled structure with its central line short-ended, a λ/4 transmission line for impedance matching, two pairs of open stub resonators as well as two isolation resistors. L_{p1}, L_{p2} and L_{p3} denote the 50-ohm feed lines. Intuitively, attributing to the symmetry of the FPD, signals excited at port 1 are expected to be equally coupled to the two side lines and then transmitted to the two output ports, i.e., port 2 and port 3 with equal magnitude and in-phase property.

To illustrate its working principles of frequency selectivity and port-to-port isolation, the even-/odd-mode analysis method is adopted herein by forcing the even-mode and the odd-mode excitations on the ports 2 and 3, respectively. For the even-mode excitation, the FPD can be equivalent to Fig. 2(a) due to no current flowing through the two isolation resistors, which can be used to decide the filtering function. While for the odd-mode, it can be divided into two identical sections displayed in Fig. 2(b) owing to an electrical wall on the symmetrical plane, which can be used to analyze the isolation and port matching

Manuscript received February 1, 2017; revised July 1, 2017.

X. Wang, J. Wang, G. Zhang, and W. Wu are with the Ministerial Key Laboratory of JGMT, Nanjing University of Science and Technology, Nanjing 210094, China (e-mail: eejpwang@gmail.com).

J.-S. Hong is with the Department of Electrical, Electronic and Computer Engineering, School of Engineering and Physical Sciences, Heriot-Watt University, Edinburgh EH14 4AS, U.K. (e-mail: j.hong@hw.ac.uk).

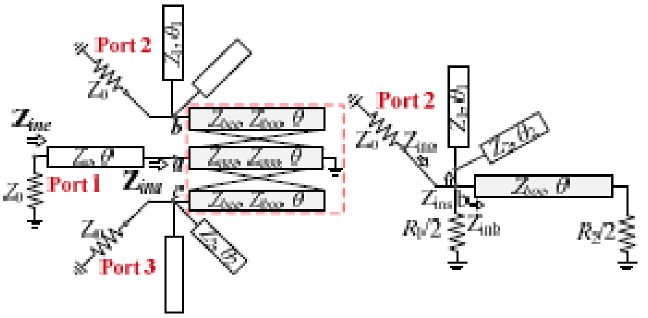

(a) (b)

Fig. 2 Equivalent circuit of the proposed FPD. (a) Even-mode equivalent circuit, (b) bisection of odd-mode equivalent circuit.

performance. Detailed analysis is given as follows.

A. Frequency selectivity

To analyze the filtering property of the proposed FPD, the input impedance at port 1 shown in Fig. 2(a) can be derived as

$$Z_{ine} = Z_a \frac{Z_{ina} + jZ_a \tan\theta}{Z_a + jZ_{ina} \tan\theta}, \tag{1}$$

where

$$Z_{ina} = Z_{aa} - \frac{2Z_{ab}^2}{Z_{bb} + Z_{bc} + Z_L}, \tag{2}$$

$$Z_L = \frac{Z_{ins} Z_0}{Z_{ins} + Z_0},\ Z_{ins} = -j\frac{Z_1 Z_2 \cot\theta_1 \cot\theta_2}{Z_1 \cot\theta_1 + Z_2 \cot\theta_2}. \tag{3}$$

Z_{mn} (m, n=a, b, c) are the impedance matrix elements of the three-port network shown in the dashed line section, which are derived as (4) according to [9].

$$Z_{aa} = j(Z_{aee} + Z_{aoo}) \tan\theta/2, \tag{4a}$$

$$Z_{ab} = Z_{ba} = Z_{ac} = Z_{ca} = j(Z_{bee} - Z_{boo}) \tan\theta/4, \tag{4b}$$

$$Z_{bb} = Z_{cc} = j[\frac{(Z_{bee} - Z_{boo})^2(1+\tan^2\theta)}{8(Z_{aee} + Z_{aoo})\tan\theta} - \frac{Z_{bee} + Z_{boo} + 2Z_{boe}}{4\tan\theta}], \tag{4c}$$

$$Z_{bc} = Z_{cb} = j[\frac{(Z_{bee} - Z_{boo})^2(1+\tan^2\theta)}{8(Z_{aee} + Z_{aoo})\tan\theta} - \frac{Z_{bee} + Z_{boo} - 2Z_{boe}}{4\tan\theta}], \tag{4d}$$

where Z_{kij} (k=a, b; ij=ee, oo, oe) are the mode impedances for the even-even, odd-odd and odd-even mode, respectively.

Ultimately, the reflection coefficient seen at port 1 can be expressed as $S_{11}=(Z_{in1}-Z_0)/(Z_{in1}+Z_0)$. Since the filtering circuit can be deemed as lossless network, the transmission coefficients can be calculated by $|S_{21}|=|S_{31}|=\sqrt{(1-|S_{11}|^2)/2}$. With $|S_{21}|$=0, three transmission zeros (TZs) are deduced as (5) over an interested band with the center frequency f_0. In this context, these TZs are successfully introduced to form the two passbands of the FPD. Fig. 3 describes the transmission response of the FPD with varied bandwidths which are controlled by the electrical lengths of the open stub resonators.

$$f_{z1} = \frac{\pi f_0}{2\theta_1},\ f_{z2} = \frac{\pi f_0}{2\theta_2},\ f_{z3} = \frac{3\pi f_0}{2\theta_1}. \tag{5}$$

As observed, by increasing the value of θ_1 or decreasing the value of θ_2, the bandwidth of first passband is expanded while the second passband is reduced. Herein, a prototype FPD operating at two passbands (2.1-2.5 GHz and 3.5-3.9 GHz) with 18 dB return loss is taken for an example. Initially, three TZs are selected at f_{z1}=1.5 GHz, f_{z2}=3 GHz, f_{z3}=4.5 GHz. Therefore, the two electrical lengths are found as θ_1=180°, θ_2=90°.

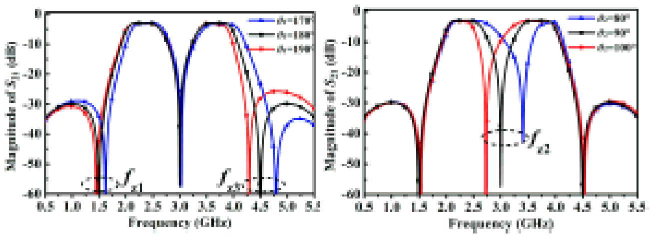

Fig. 3 Transmission responses of the proposed FPD with varied (a) θ_1, (b) θ_2.

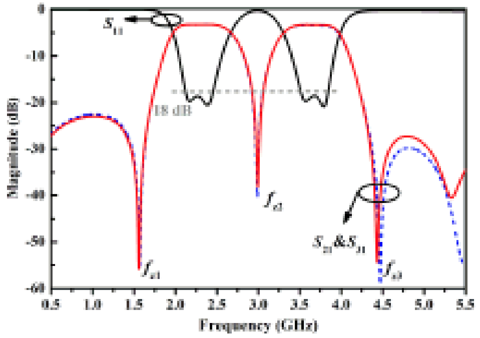

Fig. 4 The filtering response of the even-mode equivalent circuit.

To satisfy the required return loss, the mode impedances are determined as Z_{aee}=85 Ω, Z_{aoo}=20.6 Ω, Z_{bee}=260 Ω, and Z_{boo}= 127.5 Ω by optimizing the input impedance in (1) with the extracting method in [10]. According to the mapping relationship between the calculated mode impedances and dimensions illustrated in [9], the widths and gaps are obtained as W_1=0.4 mm, W_2=0.1 mm, and g=0.1 mm. Fig. 4 presents the simulation filtering response of the even-mode equivalent circuit, in which high selectivity and dual-wideband property are both achieved.

B. Port-to-port isolation

According to [4], the two output ports will be perfectly isolated at the frequency f if the odd-mode voltage reflection coefficient (Γ_o) equals to the even-mode one (Γ_e) at f. Since the $|\Gamma_e|$ has been already prescribed as the values less than 0.016 (-18 dB) at the in-band frequencies, the values of $|\Gamma_o|$ should be about 0.016 to obtain a good in-band isolation. Herein, the following odd-mode input impedance is used to calculate Γ_o.

$$Z_{ino} = \frac{Z_{ins} Z_{inb}}{Z_{ins} + Z_{inb} + 2Z_{ins} Z_{inb}/R_1}, \tag{6}$$

where

$$Z_{inb} = Z_{boe}\frac{R_2/2 + jZ_{boe}\tan\theta}{Z_{boe} + (jR_2\tan\theta)/2},\ Z_{boe} = \frac{Z_{bee} Z_{boo}(1+\varepsilon_r)}{2Z_{boo}\varepsilon_r + Z_{bee}(1+\varepsilon_r)} \tag{7}$$

Z_{boe} is the odd-even mode impedance calculated with the relative dielectric constant ε_r according to [10].

As can be seen, Z_{ino} is only related to the R_1 and R_2 at the frequency f after the mode impedances are determined. Thus, the effect of resistances variation on in-band Z_{ino} is investigated with (6)-(7), shown as Fig. 5(a). As observed, good matching can be realized with R_1 between 400 Ω and 600 Ω and R_2 around 500 Ω. Then, a parameter study partly shown as Fig. 5(b) is carried out to further confirm the resistance values. It can be

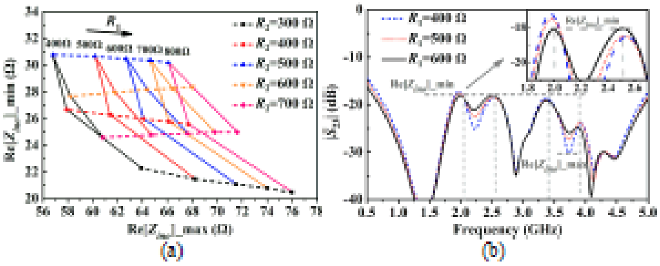

(a) (b)

Fig. 5 (a) The real part extremum of Z_{ino} within interested passbands with varied R_1 and R_2, (b) magnitude of S_{23} with varied R_1 while R_2 fixed as 520 Ω.

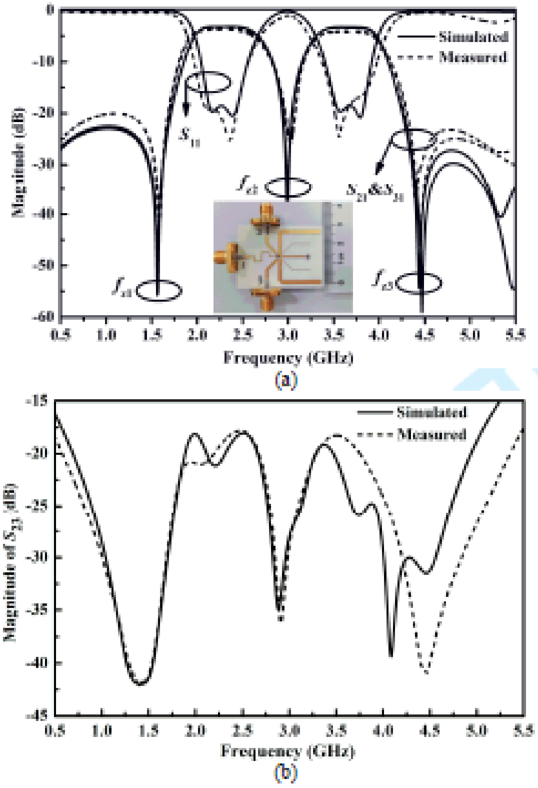

(b)

Fig. 6 Simulated and measured results of the proposed dual-wideband FPD. (a) Magnitude of S_{11}, S_{21} and S_{31}, (b) magnitude of S_{23}.

seen that with the decrease of value R_1, the maximum of in-band S_{23} keep almost constant while the minimum increases, which complies with the variation of Z_{ino} shown in Fig. 5(a). Finally, the resistances are found as R_1=600 Ω, R_2=520 Ω. In addition, it is found that outside the passbands, three transmission zeros at 1.5 GHz, 3 GHz and 4.5 GHz lead to a result of Z_{ins}=0, which causes a perfect isolation at these transmission zeros. Therefore, good isolation within a wide frequency band can be eventually realized.

III. RESULT AND DISCUSSION

The designed dual-wideband FPD is fabricated on a single layer Rogers RO4003C substrate with a dielectric constant of 3.55, a loss tangent of 0.0027, and a thickness of 0.508 mm. Final optimal dimensions (in mm) are determined as: L_1=15, L_2=7.89, L_3=8.7, L_4=9.6, L_5=18.4, L_{p1}=6, L_{p2}=6.89, L_{p3}=8.31, L_{f1}=20.9, W_1=0.4, W_2=0.1, W_3=0.1, W_4=1.6, D_1=4.87, D_2=4.79, W_p=1.18, g=0.1, with R_1=600 Ω and R_2=520 Ω. Results shown in Fig. 6 indicate that the proposed dual-band FPD operates at the center frequencies of 2.3 and 3.64 GHz with wideband 3-dB FBWs of 36.5% and 22.3%, respectively. Inside the two passbands, the measured insertion losses (ILs) are 3.8 and 4.2 dB, together with the return losses (RLs) at port 1 greater than 18.5 and 16.3 dB, simultaneously. Three finite TZs can be seen at 1.58, 3.03 and 4.45 GHz, thus resulting in high selectivity. In addition, an isolation level higher than 18 dB is obtained over a wide frequency range from 0.5 to 5.5 GHz. Table I tabulates a comparison on the performances of the proposed FPD and other reported ones. It can be seen that our proposed FPD features wide passbands and high isolation level within the entire operation bands.

TABLE I
COMPARISONS WITH OTHER PREVIOUS WORKS

Ref.	f_0 (GHz)	3-dB FBWs of dual passbands (%)	In-band isolation (dB)	In-band RL (dB)	In-band IL (dB)
[2]	1.8/2.96	11.7/11.1	>8/10	10/15	3.8/3.9
[3]	3.5/5	7.4/4.2	>8/6	13/15	3.9/4.9
[8]	2.2/2.7	12.2/8.9	>16/16	17/17	3.5/3.5
This work	**2.3/3.64**	**36.5/22.3**	**>18/18**	**18.5/16.3**	**3.8/4.2**

IV. CONCLUSION

A new dual-wideband filtering power divider (FPD) with good isolation and sharp selectivity has been presented in this letter. Its operation principle has been theoretically explained. One prototype FPD has been designed, fabricated, and measured. Both simulated and measured results indicate that the proposed dual-wideband FPD exhibits not only good filtering properties, but also a high isolation level, which is attractive for applications in modern wireless communications.

REFERENCES

[1] C. F. Chen, T. Y. Huang, T. M. Shen and R. B. Wu, "Design of miniaturized filtering power dividers for system-in-a-package," *IEEE Trans. Compon. Packag. Manuf. Technol.*, vol. 3, no. 10, pp. 1663-1672, Oct. 2013.

[2] Y. C. Li, Q. Xue and X. Y. Zhang, "Single- and dual-band power dividers integrated with bandpass filters," *IEEE Trans. Microw. Theory Techn.*, vol. 61, no. 1, pp. 69-76, Jan. 2013.

[3] Q. Li, Y. Zhang and Y. Fan, "Dual-band in-phase filtering power dividers integrated with stub-loaded resonators," *IET Microw. Antennas Propag.*, vol. 9, no. 7, pp. 695-699, May 2015.

[4] S. S. Gao, S. Sun and S. Xiao, "A novel wideband bandpass power divider with harmonic-suppressed ring resonator", *IEEE Microw. Wireless Compon. Lett.*, vol. 23, no. 3, pp. 119-121, Mar. 2013.

[5] L. Guo, A. Abbosh and H. Zhu, "Ultra-wideband in-phase power divider using stepped-impedance three-line coupled structure and microstrip-to-slotline transitions," *Electron. Lett.*, vol. 50, no.5, pp. 383-384, Feb. 2014.

[6] H. Zhu, A. Abbosh and L. Guo, "Ultra-wideband unequal in-phase power divider using three-line coupled structure," *Electron. Lett.*, vol. 50, no. 15, pp. 1081-1082, Jul. 2014.

[7] L. Guo, H. Zhu and A. M. Abbosh, "Wideband tunable in-phase power divider using three-line coupled structure," *IEEE Microw. Wireless Compon. Lett.*, vol. 26, no. 6, pp. 404-406, Jun. 2016.

[8] C. Cai, J. Wang, Y. Deng and J. L. Li, "Design of compact dual-mode dual-band filtering power divider with high selectivity," *Electron. Lett.*, vol. 51, no. 22, pp. 1795-1796, Oct. 2015.

[9] S. Yamamoto, T. Azakami and K. Itakura, "Coupled strip transmission line with three center conductors," *IEEE Trans. Microw. Theory Techn.*, vol. 14, no. 10, pp. 446-461, Oct 1966.

[10] A. M. Abbosh, "Three-way parallel-coupled microstrip power divider with ultrawideband performance and equal-power outputs," *IEEE Microw. Wireless Compon. Lett.*, vol. 21, no. 12, pp. 649-651, Dec. 2011.